

Propagation Characteristics of Liquid-Core Fibers

I: Temperature Induced Mode Cutoffs

SUSANA A. PLANAS, RAMAKANT SRIVASTAVA and ERIK I. BOCHOVE

Instituto de Física, Universidade Estadual de Campinas, São Paulo, 13.100, SP, Brasil

Recebido em :21 de Outubro de 1982

Abstract Transmitted and scattered light intensities in liquid-core fibers as a function of temperature have been measured. Several low-order mode cutoffs have been observed at temperatures which agree well with the results predicted by weakly guiding mode theory for step-index optical fibers. The results have been used to determine the core radius to a high precision. The technique described here can also be extended for monitoring temperatures in regions of difficult access or subject to large electromagnetic background.

1. INTRODUCTION

Basic theory of propagation of light in circularly symmetric optical fibers considers them as cylindrical dielectric waveguides. In optical fibers designed for communication purposes, there is a very small difference between the refractive indices of the core and cladding. If, in addition, the core refractive index is constant (step-index fiber), simplifications in theory exist which allow for a better understanding of all the propagation phenomena. However, in practice, glass fibers suffer from a series of imperfections and it is difficult to fabricate an ideal step-index fiber. On the other hand, liquid-core fibers (LCF's) are free from these imperfections and provide an excellent medium to study propagation properties of step-index fibers. Earlier work on the basic studies on LCF's can be divided in four major areas of investigation:

- (a) attenuation¹
- (b) material and modal dispersion²
- (c) selective mode launching³
- (d) polarization characteristics⁴

However, none of the work reported in these areas is related to the theoretical prediction of mode propagation in fibers. This is probably due to lack of technological interest because LCF's, although considered in the beginning for use in optical communications, have since been eliminated from the list of transmission media largely due to their

complexity and dispersion properties.

On the other hand, guiding parameters of LCF's can be varied at will by varying the temperature of a segment of the fiber. Since the refractive index of liquids is generally highly temperature dependent, the guidance properties of the fiber can be varied over relatively large range.

Thus LCF's are gifted with two major simplifications from the viewpoint of studying waveguide properties of optical fibers: (a) they are very close to a perfect step index fiber, and (b) their guidance properties can be easily varied.

In fact, a highly multimode LCF, when heated, is expected to show mode cutoffs, become single-mode in a given temperature range and finally transmit no light at all when the core refractive index equals that of the cladding. Therefore, the same fiber can be studied to obtain information about the propagation in single mode fibers with step-index profile - a situation difficult to achieve in glass fibers.

In this work, we have renewed interest in LCF's and measured transmitted and scattered radiation intensity in a liquid core fiber as its temperature was varied. Several mode cutoffs have been observed at temperatures predicted theoretically in the regime of weak guidance⁵. The values of the cutoff points have been used to determine the core radius to a high precision. It is the first study of its kind and leads to a new technique for a precise measurement of inner diameter of cylindrical capillaries. Section 2 deals with the basic theory of step-index dielectric waveguides. Experimental details are given in section 3 and the following section gives the results along with an analysis of the data. In section 5, we discuss these results and point out the merits of this technique for diameter measurement of hollow fibers.

2. THEORY

An optical fiber is made of two coaxial circular cylinders of dielectric materials. The central region is called core surrounded by the outer region called cladding. The propagation takes place in the core via total internal reflection at the core-cladding boundary. Figure 1 gives a schematic representation of a section of an optical fiber with step-index profile. In glass fibers, the interface between core and

cladding is never ideal and the refractive index profile is also never ideally a step function. Both of these deficiencies are absent in LCF's.

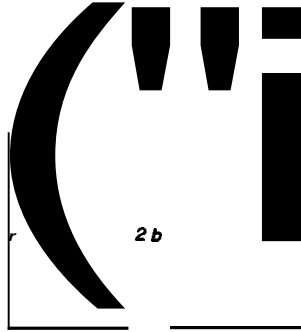


Fig.1 - Cross-section of step-index fiber.

If the refractive index difference is small, i.e.,

$$\Delta \equiv \frac{n_c - n}{n} \ll 1 \quad (1)$$

the modes that propagate are "weakly guided" and a simplified theory has been given by Gloge⁵ who denominated them LP modes because of their nearly linearly polarized character.

Consider the propagation constant β of any guided mode. It is necessary that $nk r \beta \leq n_c k$ with $k = 2\pi/\lambda$, the wavenumber in free space. If we define parameters

$$u = a(k^2 n_c^2 - \beta^2)^{1/2} \quad (2)$$

$$w = a(\beta^2 - k^2 n^2)^{1/2}, \quad (3)$$

the mode field can be expressed by Bessel function $J(ur/a)$ inside the core and modified Hankel function $K(wr/a)$ outside the core. The modes that are allowed to propagate are controlled by the value of the normalized frequency v ,

$$v^2 = w^2 + u^2 \quad (4)$$

$$v = \frac{2\pi}{\lambda} a(n_c^2 - n^2)^{1/2} \quad (5)$$

The dominant transverse Electric field components of LP modes can be

expressed as follows:

$$E_y = E_\ell \left\{ \begin{array}{l} J_\ell(ur/a)/J_\ell(u) \\ K_\ell(wr/a)/K_\ell(w) \end{array} \right\} (\cos\ell\phi) \exp\{i\omega t - i\beta z\} \quad (6)$$

The upper line holds for the core and the lower line for the cladding. The parameter E_ℓ can be expressed in terms of the power carried by the mode. The z-components of the fields are small compared to the transverse components and are combinations of the $(\ell+1)$ and $(\ell-1)$ solutions.

The characteristic equation for the LP modes is:

$$\frac{u}{n_c} [J_{\ell\pm 1}(u)/J_\ell(u)] = \pm \frac{w}{n} [K_{\ell\pm 1}(w)/K_\ell(w)] \quad (7)$$

Each mode is designated $LP_{\ell m}$; the first index ℓ corresponds to the integer that enters the circular functions and the second index m labels the roots of the characteristic equation for a given value of ℓ . Since there is a freedom of choosing either $\cos\ell\phi$ or $\sin\ell\phi$ in Eq. (6) and there are two orthogonal sets of polarization, for every $\ell \geq 1$, there are four modes. For $\ell=0$, we have only a set of two modes polarized orthogonally with respect to each other.

It must be pointed out that in dielectric waveguides all but the cylindrical symmetric modes ($\ell=0$) are hybrid, i.e. they have both non-zero electric and magnetic z components. Each mode $LP_{\ell m}$ contains modes which can be identified as $HE_{\ell+1,m}$ and $EH_{\ell-1,m}$ or TE_{0m} and TM_{0m} . If E_z is larger than H_z , the mode is designated $EH_{\ell m}$, otherwise $HE_{\ell m}$. The propagation constants of $HE_{\ell+1,m}$ and $EH_{\ell-1,m}$ are almost identical and in the limit $n_c \rightarrow n$, the two are degenerate and the characteristic equation (7) takes the form:

$$u [J_{\ell-1}(u)/J_\ell(u)] = -w [K_{\ell-1}(w)/K_\ell(w)] \quad (8)$$

Setting $w=0$ yields the cutoff values $J_{\ell-1}(u_c) = 0$. In general, solution of Eq. (8) is non analytical. However, to a good approximation⁵,

$$u = u_c \exp\{\text{arc sin}(s/u_c) - \text{arc sin}(s/v)\}/s \quad (9)$$

where

$$s = (u_c^2 - \ell^2 - 1)^{1/2} \quad (10)$$

Eq. (9) is valid for all modes except the $LP_{0,1} = HE_{1,1}$ mode in which case:

$$u \approx (1+\sqrt{2})v / [1+(4+v^4)]^{1/4} \quad (11)$$

If now we define parameter b as a normalized propagation constant given by

$$b(v) \approx \frac{(\beta/k - n)}{(n_c - n)} \quad (12)$$

one can plot $b(v)$ curves as a function of the normalized frequency v . Figure 2 shows these curves which have been obtained numerically for the

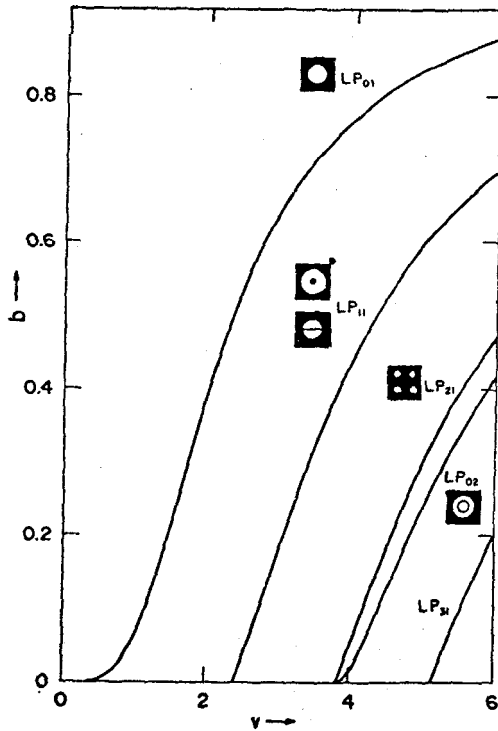


Fig.2 - b vs v curves for some low-order modes in weakly guiding mode theory, with the lower order mode patterns as seen in the near-field.

lowest five LP modes. It can be clearly seen that a mode can be guided only above certain limiting v -value which is given by $v_c = u_c$ shown in Table 2. Thus if v -value of a fiber is varied by either varying the wavelength λ of the radiation^{6,7} or the refractive index n_c of the core

material, as in our case, Eq. (5) shows that the respective values of v_c can be measured and compared with those listed in Table 2.

Table 1 - Characteristics of the fibers used.

Fiber	Core radius (μm)	Liquid	$n_D(20^\circ\text{C})$	$\frac{dn}{dT} [^\circ\text{C}^{-1}]$
C,D,E	5.5	Light Paraffin	1.4640	-3.7×10^{-4}
B,F	5.8	Light Paraffin	1.4640	-3.7×10^{-4}
A	6.0	Heavy Paraffin	1.4700	-3.6×10^{-4}

Table 2 - Theoretical and Experimental v -values and the corresponding core-radius values for each cutoff.

LP MODE	v_{CT}	FIBER	v_{CE}	$a [\mu\text{m}]$
$LP_{11} \left\{ \begin{array}{l} HE_{21} \\ HE_{01} TM_{01} \\ HE_{01} TE_{01} \end{array} \right.$	2.405	C	2.5	5.3
		D	2.6	5.1
		E	2.5	5.3
		B	2.4	5.8
		F	2.5	5.6
		A	2.6	5.6
$LP_{02} HE_{12}$ $LP_{21} \left\{ \begin{array}{l} HE_{31} \\ HE_{11} EH_{11} \end{array} \right.$	3.832	C	4.2	5.0
		D	4.0	5.3
		E	3.9	5.4
		B	3.8	5.8
		F	3.8	5.8
		A	4.0	5.7
$LP_{31} \left\{ \begin{array}{l} HE_{41} \\ HE_{21} EH_{21} \end{array} \right.$	5.136	C	-	-
		D	5.2	5.4
		E	5.2	5.4
		B	5.2	5.7
		F	5.2	5.7
		A	-	-

3. EXPERIMENTAL

Fibers used in this work were one to two meters in length, $80\mu\text{m}$ in cladding diameter and approximately $11\mu\text{m}$ in internal diameter. The cladding material was quartz and the characteristics of the fibers used are given in Table 1. The liquid to fill the fiber, must be chosen to satisfy the condition of optical guidance, i.e., the refractive index of the liquid must be higher than that of the quartz cladding [n at $6328\text{ \AA} = 1,457$]. Heavy and light paraffin were used in this work.

A. Filling Process

The hollow fibers were filled under hydrostatic pressure using an apparatus which is shown in Fig. 3 and is basically the same as described by Stone⁵.

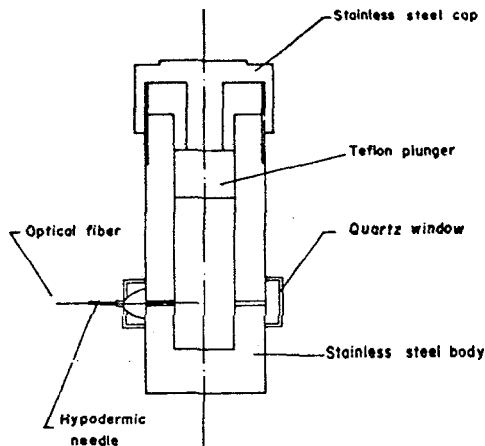


Fig.3 - Apparatus for filling the fibers.

The fiber was held in place by passing it through a hypodermic needle which was then attached to a lower lock hypodermic syringe fitting attached to the filling cell. The fiber was epoxied at the end of the hypodermic needle. Care was taken not to introduce any bubbles in the liquid.

To obtain fiber end faces of optical quality, it was found convenient to break the fiber while under tension. However the fiber could

also be cut without apparatus, simply with the curvature of the finger and a cutting element such as diamond. In every case, both ends were checked under a microscope, to be sure to have a reasonably plane optical surface free of any broken pieces to avoid scattering problems.

B. Refractive Index Measurements

To measure the refractive index of the liquids, a critical angle refractometer (Abbe^{3L} refractometer of Bausch & Lomb) was used. Water was circulated in its prism cases, and its temperature was varied from 20° to 60° with the help of a controller. The temperature readings were made by using an internal thermometer. Fig. 4 shows the variation of the refractive index at the sodium D-line with temperature for the heavy paraffin (curve II) and for the light paraffin (curve I). Table I gives the values of $|\frac{dn}{dT}|$. As expected, the refractive index varies linearly with temperature. The accuracy in the n_D measurement is of $\sim 2 \times 10^{-4}$. The refractive index of fused quartz can be considered relatively constant ($|\frac{dn}{dT}| = 3 \times 10^{-6} \text{ } ^\circ\text{C}^{-1}$). Assuming linear dispersion, the refractive index of the liquid was corrected to the He-Ne wavelength. The necessary correction is given by the equation:

$$n_{\text{He-Ne}} = n_D + \frac{dn}{d\lambda} \Delta\lambda = n_D - 0.0023 ,$$

where $\frac{dn}{d\lambda}$ was measured by the refractometer.

C. Launching Conditions

It has been shown by Gambling et al.⁹ that by careful adjustment of the launching conditions, a desired set of modes can be excited. The method employed for selective mode excitation is as follows. The fiber is maintained at a temperature corresponding to a v -value just above the cutoff point of the desired mode. At this point the launching conditions were adjusted using angular and translational movements of the fiber end until the power coupled reached a maximum. Convenient identification of the mode or combination of coupled modes was made by inserting a polarizer and analyser in the light path¹⁰. Some of the mode patterns are shown in Fig. 2. The efficiency reached for excitation of the fundamental mode was 60%.

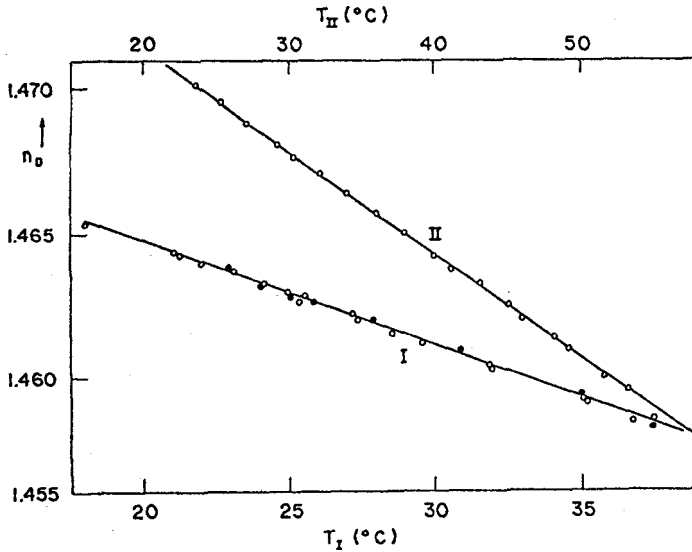


Fig.4 - Variation of refractive index of two paraffins with temperature.

D. Experimental Arrangement

The experimental arrangement used for measurements of transmitted and scattered intensity is shown in Fig. 5.

A He-Ne laser, Spectra Physics 125A, operating in single transverse mode TEM_{00} with 50 mW of power was used as a source. The input beam passes through a beam splitter to produce a reference signal and a variable neutral density filter, which gives the variable power when required. Typical power input was of the order of few mW. A power objective lens (Zeiss 10x, NA25), mounted in a XYZ micropositioner was used to focus the beam into the fiber. The entrance end of the fiber is inserted into a liquid cell (Fig. 6), filled with the same paraffin as the fiber. The windows of the entrance cell are made from microscope-slide-covers. The cell acts as a reservoir for the liquid avoiding its leakage from the fiber, and it also strips out the cladding modes. The fiber can be easily pushed until it touches the window and then cemented to the capillary glass tubing. The cell is mounted into angular and XYZ micropositioners which permit fine adjustment of the beam focus into the core of the fiber. The output of the fiber is inserted again in an identical paraffin cell. The fiber passes through a temperature con-

trolled furnace of 21 cm of length.

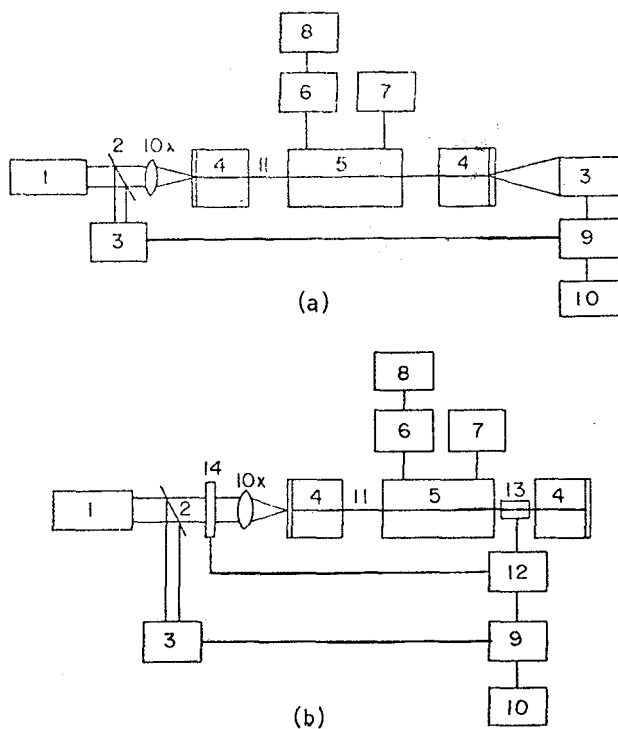


Fig.5 - Experimental arrangement for (a) transmission and (b) scattering measurements.

1 - He-Ne Laser; 2 - Beam Splitter; 3 - Power Meter; 4 - Liquid Cell; 5 - Furnace; 6 - Thermocouple; 7 - Temperature Controller; 8 - Digital Voltimeter; 9 - Voltage Divider; 10 - Chart Recorder; 11 - Fiber; 12 - Lock-in Amplificator; 13 - Pin-Detector; 14 - Chopper.

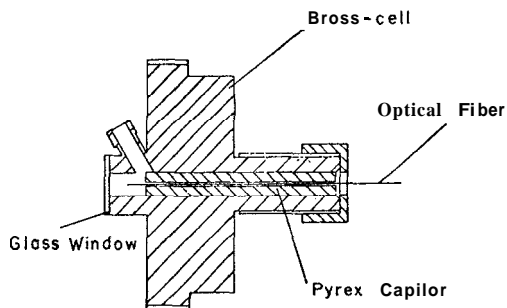


Fig.6 - Schematics of the liquid cell.

Fig. 7 shows the furnace which consists of two concentric cylinders. The fiber passes through the inner copper cylinder, containing dark oil to quickly remove any cladding radiation due to temperature-induced mode cutoffs. A thermocouple, (junction of nichel chromium vs ni-

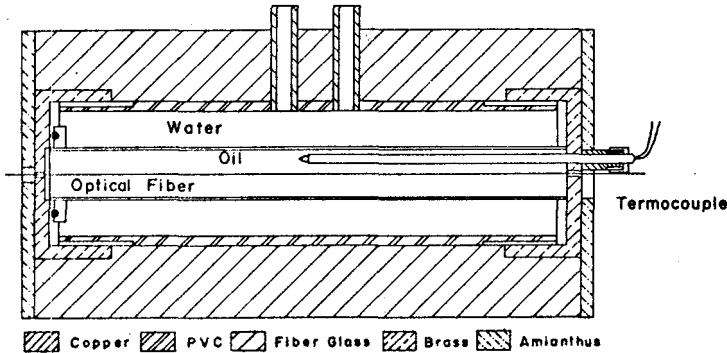


Fig.7 - Liquid-heated Furnace.

chel aluminium) immersed in this liquid measures the temperatures. In the space between the two cylinders water of controlled temperature was circulated. The heating rate, below 0,5C/min., was sufficiently slow such that the system could be maintained in quasi-thermal equilibrium. It must be pointed that the temperature variation was not linear in time but it was sufficiently close to linear to allow measurements of the cutoff points with high precision.

The fiber was maintained straight all along its length, and the part before the furnace was supported in a V-groove which contained a blackoil. This removes the cladding radiation and also functions to prevent movement of the fiber and to assist in maintaining a uniform temperature. Maintaining the fiber steady is essential in order to limit modal noise (unsteady speckle pattern) caused by changes in the intermodal delays due to vibration - induced mechanical distortion in the fiber.

Fig. 5(a) shows the experimental arrangement for the transmitted intensity measurements. It was detected by a power meter (Coherent radiation model 212), placed next to the window of the exit liquid-cell. The reference intensity was measured by a radiometer and fed to

the voltage divider to correct for laser intensity fluctuations. The signal of the divider was recorded on a strip chart recorder. Fig. 5(b) shows the scattered-power measurement configuration. Essentially it is the same as in the case of the transmitted intensity and can also be monitored simultaneously. A two-cms segment of the fiber between the furnace and the exit liquid cell is placed between two large area silicon-photodetectors and immersed in paraffin which efficiently couples the radiated light to the detector. The input beam was chopped and the electronics is the one typically used for low-noise signal, using a lock-in amplifier.

In most cases, transmitted and scattered intensities were measured simultaneously. Measurements were done during the heating as well as the cooling process in order to check for the reproducibility of the results.

4. RESULTS

Fig. 8 shows the transmitted (upper curve) and scattered (lower curve) intensity patterns measured in Fiber F. As mentioned earlier, the abscissa is linear in time but only approximately linear in temperature. The corresponding v -values denoted in the upper part of the figure were calculated by inserting the respective values of A , α , n , and n_c in Eq. (5). The corresponding values of n_c were obtained from the n_c vs T curves (Fig. 4). In figure 8, the transmitted intensity shows regions where the intensity is almost constant. As the temperature is increased, the v -value decreases. As the cutoff point of a certain mode is approached, leakage of power from core to cladding occurs and the transmitted intensity shows a drop. As the temperature is increased further, the decay in the intensity is no longer observed and another flat region starts showing the guidance of the remaining modes. The cutoff experimental v -value (v_{CE}) is assigned to the point where no transmitted intensity is detected in the respective mode. Fig. 8 shows four such flat regions and four cutoff points corresponding to the LP_{12} , LP_{02} , LP_{11} and LP_{01} mode cutoffs respectively.

It must be emphasized that theoretically, the LP_{01} mode has cutoff at the temperature where the refractive index of the liquid equals that of the cladding material. However, in practice, very little light

reaches the detector near temperatures corresponding to $v \approx 1,0$ where for practical purposes the field is no longer guided¹¹. Apart from the observation of the mode cutoffs, the transmission curve in Fig. 8 shows

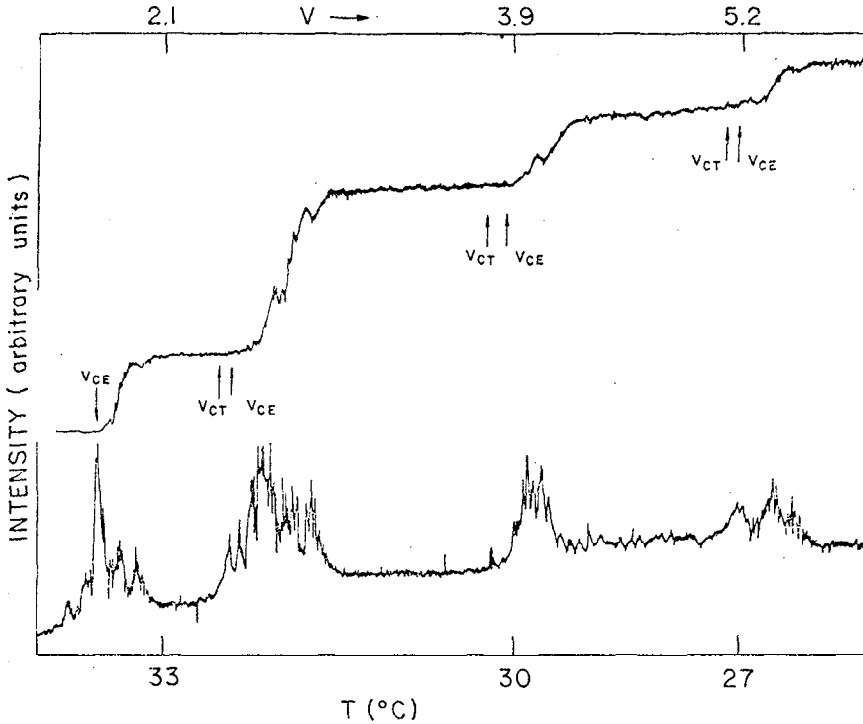


Fig.8 - Transmitted (upper curve) and scattered (lower curve) intensities vs. temperature and v -value for fiber F.

three main features which should be pointed out.

- (a) The drop in the intensity at a mode cutoff point is not abrupt but shows a gradual behavior.
- (b) The theoretical v_c values (v_{CT}) are always lower than the experimental values (v_{CE}), although the difference is very small.
- (c) There are sharp spikes present near the cutoff region whenever the removal of the cladding radiation in the furnace is incomplete. When a conventional air furnace was used with no mechanism to remove cladding radiation within the furnace, these spikes were abundant in the data, causing difficulty in identification of cutoff points. However, when the fiber was placed in the liquid oven, these vari-

ations were much smaller, indicating that they were caused by the cladding radiation.

The features (a) and (b) will be explained in the next section when we discuss our results.

The scattered intensity variation in Fig. 8 shows peaks in the curve near the mode cutoff points. These peaks correspond to the power coupled to the cladding when the mode is not guided. The peak positions match with the temperature values corresponding to the decrease in the transmitted intensity. Therefore; a precise determination of the peak positions may give accurate values of the cutoff points. However, as may be seen in the data, each such peak has a rather complex structure which does not permit such a precise measurement of the v_c values. The origin of this structure lies in the fact that the photodetectors to measure the scattered light signal produced microbending of the fiber causing it to be highly sensitive to any small fluctuations in the mechanical stability of the experimental arrangement or to small temperature fluctuations which may have occurred during the experiment. Therefore, we believe that the transmission data gives more accurate values of v_{CE} .

The identification of the mode cutoffs was also confirmed by simultaneous observation of the near-field mode patterns¹⁰ as mentioned in Section 3C. At the points where the transmitted intensity showed sudden decrease and the scattered intensity increased, it was possible to observe the unguided mode disappear at the exit end of the fiber.

Figs. 9 and 10 show transmitted intensity behavior for Fibers E and D respectively. The same feature as described earlier are observed here also. In every case, the agreement between v_{CT} and v_{CE} for each mode is reasonably good. Besides the mode cutoffs, one observes oscillations. This behavior is discussed elsewhere¹².

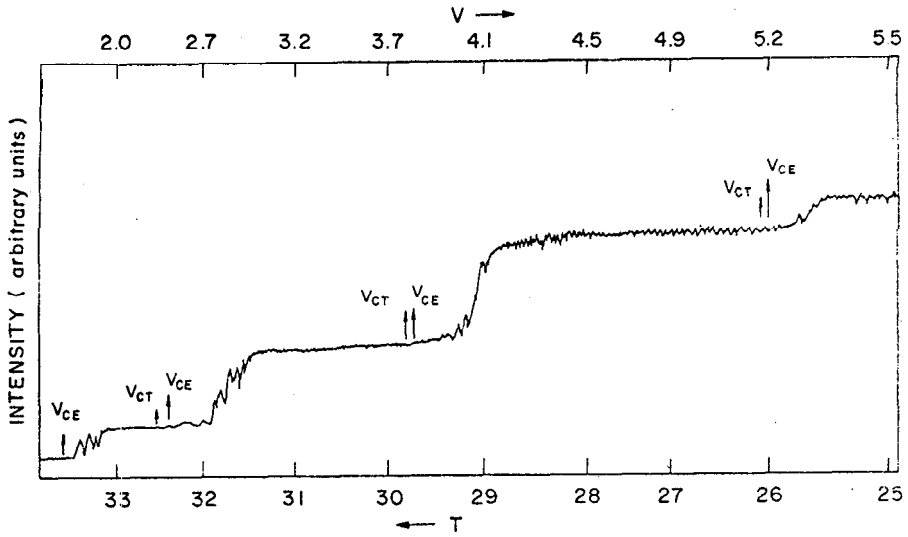


Fig.9 - Transmitted intensity vs. temperature and v-value for fiber E.

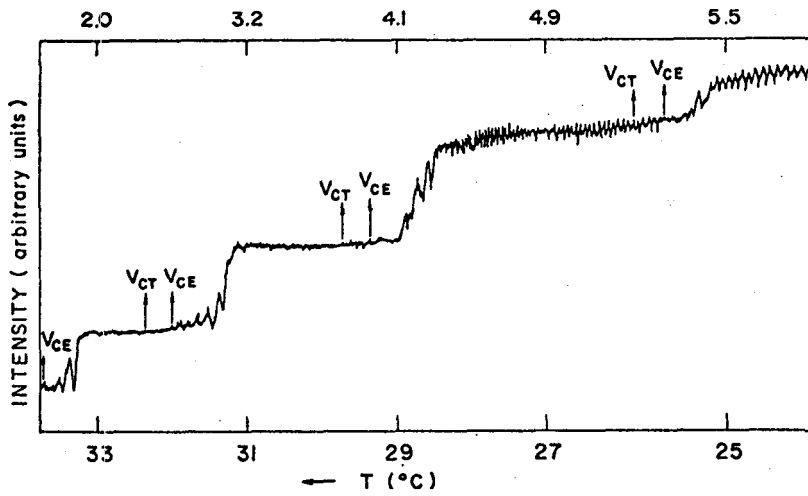


Fig.10 - Transmitted intensity vs. temperature and v-value for fiber D.

5. DISCUSSION

As mentioned earlier, three simultaneous observations were used to identify mode cutoffs as a function of temperature. It is possible to reproduce the values of the cutoff temperatures for the various modes with a precision of better than 0.1°C . However, the precision in the experimental v values (v_{CE}) is not that favourable because of the limited precision in the determination of the $n_c(T)$ curve using the refractometer. Nevertheless, this error is not very large at lower temperatures where n_c has relatively large value, but it may become serious as n_c approaches n where the difference $(n_c^2 - n^2)$ in Eq. (5) cannot be evaluated with great precision. This trend can be inferred from the Table 2 which gives the v_{CT} and v_{CE} values in various cases. It can easily be seen that, in most cases, the theoretical v_c values lie lower than the corresponding experimental values. This is not surprising. In the case of characterization of single mode fibers for the determination of wavelength corresponding to the cutoff of the LP_{11} mode, similar results have been reported¹³. The effect has been related to the fiber imperfections and bending effects¹³. We have tried to minimize these effects in LCFs by keeping the fibers fairly straight. The observed cutoff being gradual and not abrupt is also related to the above mentioned factors.

The experimental cutoff temperatures indicated by arrows in Figs. 8, 9 and 10 can be used to calculate the core radius \underline{a} if we assume that they correspond to the theoretical cutoff v -value given by the weakly guiding mode theory. In table 2, the core-radius \underline{a} has been calculated for various cutoffs in many fibers using Eq. (5). The value of \underline{a} obtained for each cutoff differs from that given in Table 1 which presents nominal values as measured by an optical microscope. Since diffraction effects limit the resolution, the values in Table 1 have lower precision limited to the resolution of one-half the wavelength of the radiation used. On the other hand, the average \underline{a} value given by data in Table 2 has a better precision.

The technique of temperature dependent mode cutoffs described here in the LCF's can be extended to monitor temperature in regions where either the presence or magnitude of strong electromagnetic background does not permit the use of conventional current sensors. The liquid in the core can be chosen so as to cut off a lower order mode at

the desired temperature, whereby the sudden change in the transmitted or scattered intensity can be monitored to detect small temperature variations around the set temperature.

6. CONCLUSION

By varying the temperature of a liquid-core fiber, we have measured variations in the transmitted and scattered intensity which have been related to the predictions of the weakly guiding mode theory. In particular, we have measured several mode cutoff temperatures whose values agree well with the theoretical predictions. The results show that the studies provide a new technique for measurement of core-radius in hollow fibers and can be extended to monitor small variations in temperature in regions of difficult access or subject to electromagnetic interference.

We acknowledge technical help of Danilo Dini. This work was supported by TELECOMUNICAÇÕES BRASILEIRAS S/A (TELEBRÁS).

REFERENCES

1. D. Payne, W. Gambling, *Electron. Lett.* 8, 375 (1972).
2. W. Gambling, D. Payne and H. Matsumura, *Opt. Comm.* 6, 317 (1972).
3. W. Gambling, D. Payne and H. Matsumura, *Electron. Lett.* 9, 412 (1973).
4. Papp and Hams, *Appl. Opt.* 16, 1315 (1977).
5. D. Gloge, *Appl. Opt.* 10, 39 (1971).
6. R. Worthington, *J. Phys. E4*, 1052 (1971).
7. J.E. Midwinter and M.H. Reeve, *Opto-Electronics* 6, 411 (1974).
8. J. Stone, *IEEE J. Quantum Elect.* QE 8, 386 (1972).
9. W.A. Gambling, D.N. Payne and H. Matsumura, *Electron. Lett.* 9, 412 (1973).
10. E. Snitzer and H. Oesterberg, *J. Opt. Soc. Am.*, 51, 499 (1961).
11. D. Marcuse, *Light Transmission Optics*, Van Nostrand, Princeton, N.J., U.S.A., 1972.
12. Susana A. Planas, Ramakant Srivastava and Erik Bochove, to be published.

13. W.A. Gambling, D.N. Payne, H. Matsumura and S.R. Norman, *Electron. Lett.* 13, 134 (1977).

RESUMO

Foram medidas intensidades de luz transmitida e espalhada em fibras de núcleo líquido em função da temperatura. Foram observados cortes de vários modos de baixa ordem à temperaturas que correspondem bem aos resultados previstos pela teoria de guiamento fraco em casos de índice degrau. Os resultados foram usados para determinar o raio do núcleo com alta precisão. Esta nova técnica também pode ser estendida para monitorar temperaturas em regiões de difícil acesso ou sujeitas a grandes ruídos gerados por campos eletromagnéticos.